

Supplemental Figures Legends

Supplemental Figure 1. Occludin does not regulate general small intestinal architecture, proliferation, or migration.

A. H&E-stained sections show normal organization of crypt-villus units in occludin KO mice.

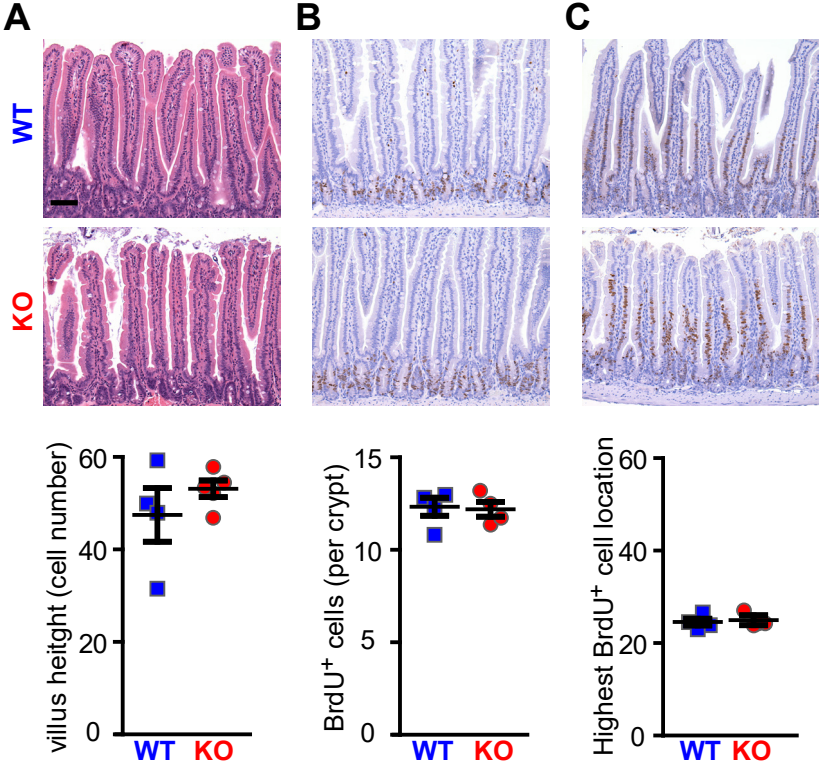
There was no difference in number of cells per villus. Bar = 100 μ m (n = 4-5 per genotype).

B. BrdU staining of small intestine harvested 2 hours after BrdU injection. There was no difference in number or location of BrdU incorporating cells between KO and WT mice. Bar = 100 μ m (n = 4 per genotype).

C. BrdU staining of small intestinal tissue sections from mice injected with BrdU 24 hours before sacrifice. Migration of BrdU cells was not altered by occludin KO. Bar = 100 μ m (n = 3-4 per genotype).

All statistical analyses were non-significant ($P > 0.05$) by Student's *t*-test.

Supplemental Figure 1



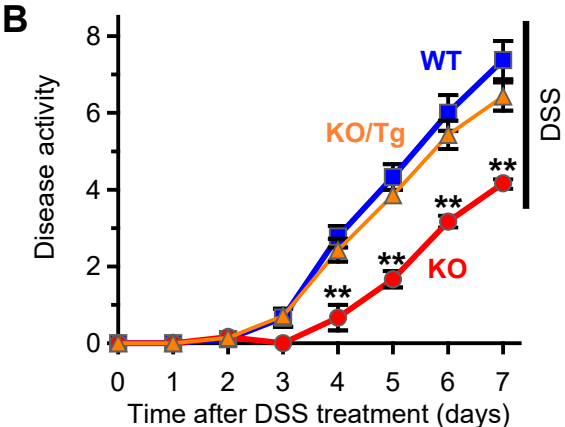
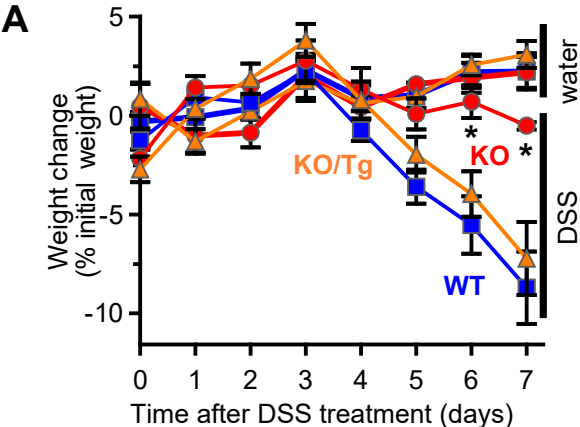
Supplemental Figure 2. Occludin KO limits severity of DSS colitis.

A. Weight loss following DSS treatment was attenuated by occludin KO. Sensitivity to DSS was restored by transgenic intestinal epithelial EGFP-occludin expression. (n≥3 for water groups and n≥4 for DSS-treated groups). Additional data are shown in Fig. 1A.

B. Disease activity scores were reduced in occludin KO mice (n≥6 per group). Additional data are shown in Fig. 1B.

Statistical analyses by one-way ANOVA with a Bonferroni post-test; *, P<0.05; **, P<0.01.

Supplemental Figure 2

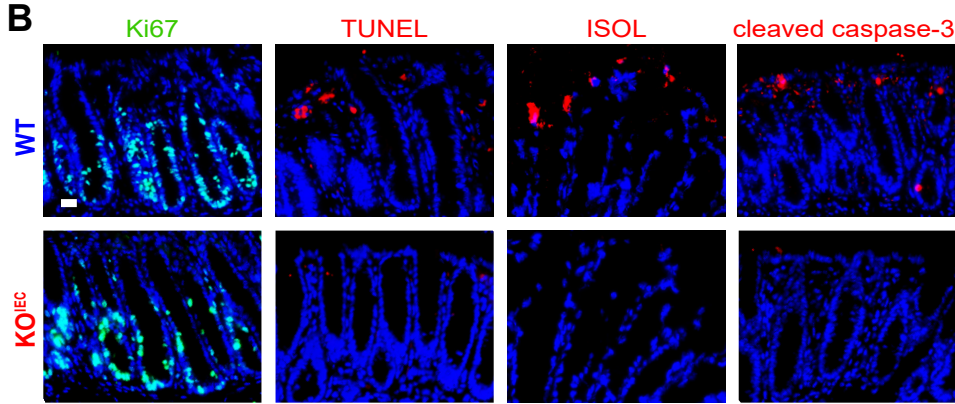
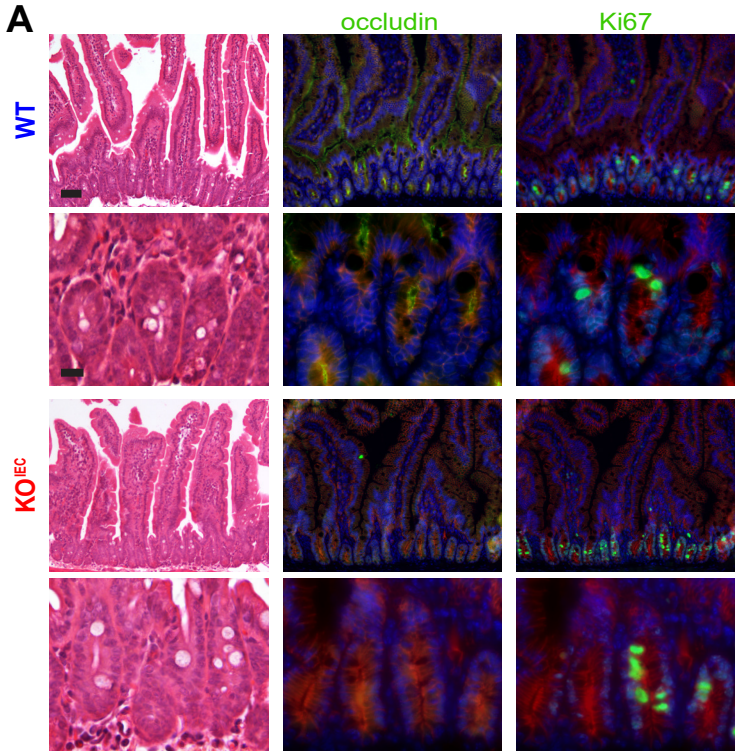


Supplemental Figure 3. Epithelial occludin expression does not impact basal small intestinal or colonic homeostasis, but facilitates TNBS-induced apoptosis.

A. H&E-stained sections show normal mucosal organization in jejunal mucosa of occludin KO^{IEC} mice. There was no difference in number of cells per crypt-villus unit. E-cadherin (red) expression was unaffected in occludin KO^{IEC} mice (occludin is shown in green). Ki67 staining (green) of the same field shows similar numbers of positive cells within crypts of WT and KO^{IEC} mice. Nuclei are shown in blue. Bars = 50 μ m (low magnification), 20 μ m (high magnification).

B. TNBS increased colonic epithelial proliferation similarly in WT and occludin KO^{IEC} mice (Ki67, green). TNBS increased numbers of TUNEL-positive (red), ISOL-positive cells (red), and cleaved caspase-3-positive (red) cells in WT, but not occludin KO^{IEC}, mice. Nuclei are shown in blue. Bar = 50 μ m Additional data are shown in Fig. 2F-I.

Supplemental Figure 3



Supplemental Figure 4. Caspase-3 expression and reduced TNF-induced caspase-3 cleavage are specific to occludin KO mice.

A. Phospho-ERK (pERK) to ERK densitometry ratios for jejunal epithelia isolated from vehicle- or TNF-treated WT and occludin KO mice (n = 3 per group). Additional data are shown in Fig. 3H,

B. Phospho-p38 (pp38) to p38 densitometry ratios for jejunal epithelia isolated from vehicle- or TNF-treated WT and occludin KO mice (n = 3 per group). Additional data are shown in Fig. 3H,

C. Densitometry of I κ B expression in jejunal epithelia isolated from vehicle- or TNF-treated WT and occludin KO mice (n = 3 per group). Additional data are shown in Fig. 3H.

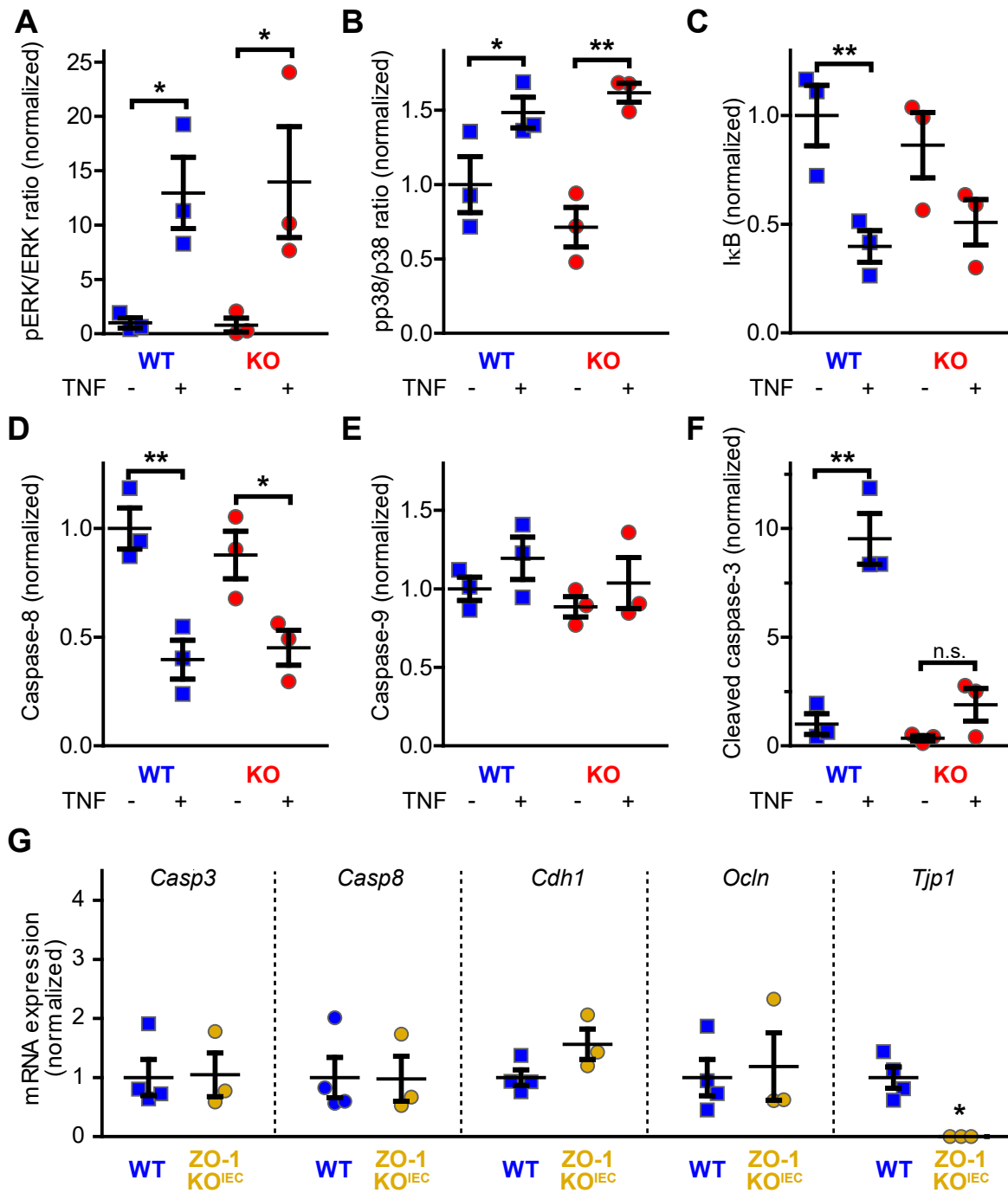
D. Densitometry of caspase-8 expression. Additional data are shown in Fig. 3H.

E. Densitometry of caspase-9 expression. Additional data are shown in Fig. 3H.

F. Densitometry of cleaved caspase-3. Additional data are shown in Fig. 3H.

G. qRT-PCR using RNA from colonic epithelial cells isolated from WT and intestinal epithelial-specific ZO-1 knockout (ZO-1 KO^{IEC}) mice. ZO-1 deletion had no effect on *Casp3* mRNA abundance. *Casp8*, *Cdh1*, and *Ocln* expression were also unaffected (n = 5 per group).

Supplemental Figure 4



Supplemental Figure 5. Occludin regulates intestinal epithelial cell apoptosis in vitro.

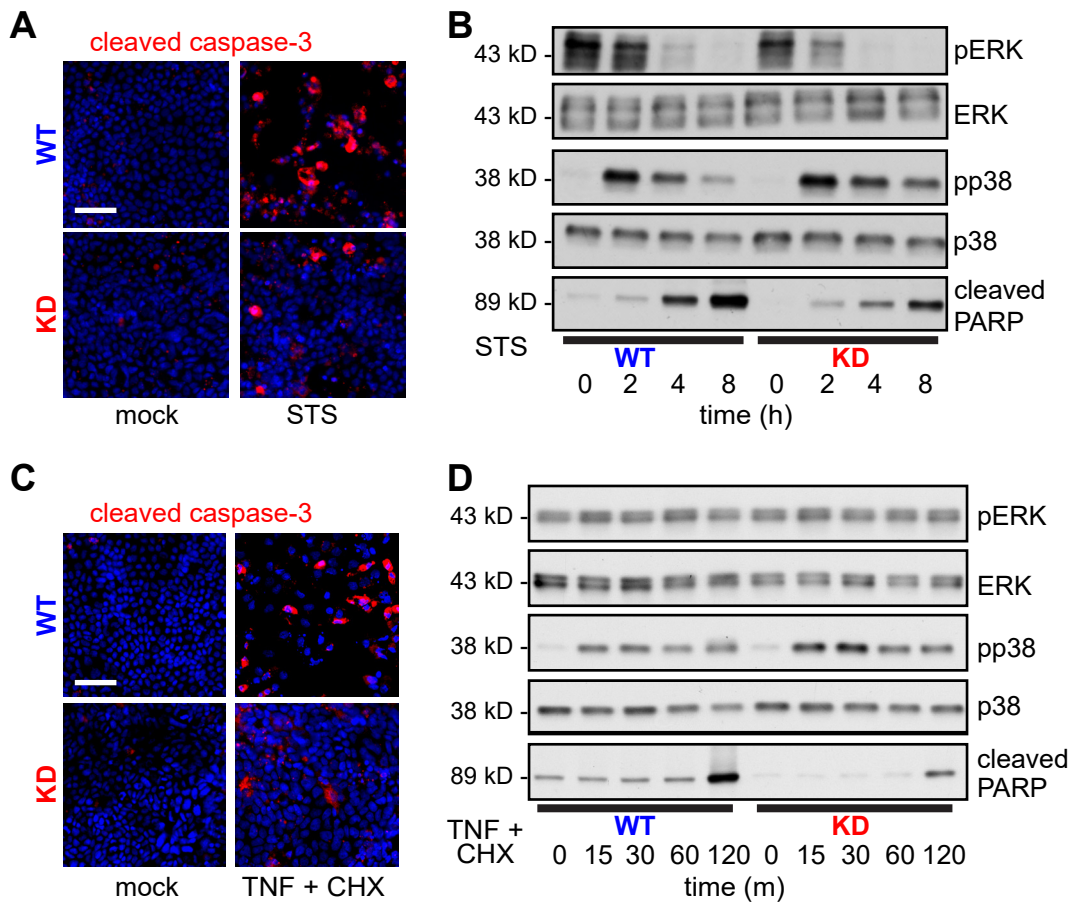
A. Apoptosis induced by staurosporine (STS), as indicated by cell loss and caspase-3 cleavage (red), was suppressed in occludin KD Caco-2_{BBE} monolayers. Nuclei are shown in blue. Bar = 100 μ m.

B. Western blots show similar STS-induced decreases in ERK and increases in p38 phosphorylation in WT and occludin KD monolayers. In contrast, STS-induced PARP cleavage was reduced in occludin KD monolayers.

C. Apoptosis induced by TNF and CHX, as indicated by cell loss and caspase-3 cleavage (red), was suppressed in occludin KD Caco-2_{BBE} monolayers. Nuclei are shown in blue. Bar = 100 μ m.

D. Western blots of TNF and CHX-treated control and occludin KD Caco-2_{BBE} monolayers show similar p38 phosphorylation. In contrast, TNF and CHX-induced PARP cleavage was reduced in occludin KD monolayers.

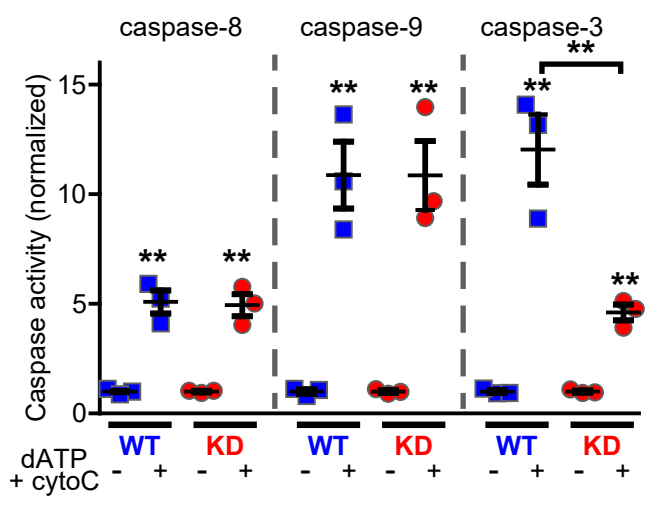
Supplemental Figure 5



Supplemental Figure 6. Occludin regulates caspase-3 activity. Fluorogenic assays were used to measure caspase-8, -9, and -3 activity induced by deoxyadenosine triphosphate (dATP) and cytochrome C. Caspase-8 and -9 activities were similar in cytosol from WT and occludin KD Caco-2_{BBE} monolayers. In contrast, caspase-3 activity was reduced in occludin KD lysates (n = 3 per group).

One-way ANOVA analysis with Bonferroni post-test. **, P<0.01.

Supplemental Figure 6



Supplemental Figure 7. Colonic tissues from ulcerative colitis patients have decreased occludin and caspase-3 expression.

A. H&E and immunohistochemical stains of colonic biopsies show decreased expression of occludin and caspase-3, but not E-cadherin, in the intestinal epithelium of ulcerative colitis patients, relative to normal subjects. Bar = 50 μ m.

B. Semi-quantitative analysis of staining intensity (n = 17 ulcerative colitis, n = 7 normal) shows significantly reduced occludin and caspase-3, but not E-cadherin, expression in ulcerative colitis.

C. Caspase-3 expression correlated with occludin expression ($r^2 = 0.71$).

Statistical analysis by Mann-Whitney U test. *, P<0.05; **, P<0.01.

Supplemental Materials and Methods

Mouse and human samples

Occludin KO (*Ocln*^{tm2Sts}, MGI:3582579),¹ intestinal epithelial specific EGFP-occludin transgenic (*Tg(Vil1-EGFP/Ocln)#Tj*, MGI:5584102),² villin-Cre (*B6.Cg-Tg(Vil1-cre)20Syr*, MGI:3053819),³ caspase-3 KO (*Casp3*^{tm1Flv}, MGI:2158753),⁴ and ZO-1 KO^{IEC} (*Tjp1*^{ff} x villin-Cre)⁵ mice have been described previously. Mice with intestinal epithelial-specific occludin deletion were generated using *Ocln*^{tm1a(KOMP)Wtsi} ES cells (Wellcome Trust Sanger Institute, MGI:4433791) with *Flp* transgenic mice (*B6.Cg-Tg(ACTFLPe)9205Dym/J*, MGI: 2448985) to delete the *En2SA-LacZ-neo* cassette between the Frt sites, thereby creating the *Ocln*^{ff} mice (after elimination of the *Flp* transgene). B6-*Ocln*^{ff} mice were crossed with villin-Cre mice to generate occludin KO^{IEC} mice for experimental use. Littermate *Ocln*^{ff} mice that lacked the *Cre* transgene were used as wild type controls in all experiments that analyzed occludin KO^{IEC} mice. Male and female 8-14 week old mice were used for experiments. All mice were maintained on C57BL/6J backgrounds under specific pathogen free conditions with 12 hour light-dark cycles. Mouse studies were performed under protocols approved by the University of Chicago, Brigham and Women's Hospital, or Boston Children's Hospital Institutional Animal Care and Use Committees.

Murine TNF (7.5 µg/mouse Peprotech), anti-CD3 IgG (200 µg/mouse, clone 2C11, BioXCell),⁶ 5-FU (200 mg/kg, MilliporeSigma), BrdU (50 mg/kg, MilliporeSigma) were administered by intraperitoneal injection. DSS (3%) was including in drinking water for 7 days. TNBS colitis was induced by skin pre-sensitization with 0.15 ml of 1% (w/v) TNBS solution in water/acetone/olive oil (16:4:5) and, 1 week later, intrarectal administration of 0.1 ml of 2.5% TNBS (w/v) in 50% ethanol.⁷ For DSS and TNBS colitis, disease activity scores were determined using a 10 point scale in which a score of 0, 1, or 2 was given for activity, posture, fur texture, stool consistency, and fecal blood. Gross photos were collected using a D90 camera with 40mm F2.8 AF-S DX micro Nikkor lens and ring light. Dissected intestinal tissues were fixed in 10% neutral buffered formalin for paraffin embedding, snap-frozen in optimal cutting temperature (OCT) media, frozen in RLT buffer (Qiagen) for qRT-PCR analyses, or used for intestinal epithelial cell isolation, as below.

De-identified patient biopsies were obtained from the archives of Brigham and Women's Hospital and University of Chicago Departments of Pathology under IRB-approved protocols. Only ileal biopsies from patients with established histories of Crohn's disease or left-sided biopsies from patients with established histories of ulcerative colitis were considered. Biopsies

with extensive ulceration were excluded. Ileal and left-sided colon biopsies without abnormalities from otherwise healthy patients undergoing screening colonoscopies were used as controls.

Intestinal epithelial cell culture and monolayer treatment

Caco-2_{BBE} derived clones, including control and occludin KD cells,⁸ were maintained in DMEM supplemented with 4.5g/L D-glucose (Corning), 10% fetal bovine serum (ThermoFisher), and 15 mM HEPES. Cells were plated on Transwell supports (Corning), as described.^{8,9} For TNF treatment, monolayers were pretreated with recombinant human interferon- γ (10 ng/ml, Peprotech) basolaterally for 18–24 h to induce TNF receptor expression, as previously described⁹. Low-dose human TNF (0.5 ng/ml, Peprotech) or high-dose human TNF (50 ng/ml) with cycloheximide (20 μ g/ml) were added to basolateral chambers as described for each experiment⁹. Staurosporine (2 μ M, Cell Signaling) was added to both apical and basolateral chambers.

Immunostaining and microscopy

Paraffin embedded tissues were deparaffinized and underwent antigen retrieval in a pressure cooker using pH6 citrate buffer. After blocking, sections were stained with antibodies against occludin (ThermoFisher 33-1500), caspase-3 (Cell Signaling 9662), cleaved caspase-3 (Cell Signaling 9664), Ki67 (Abcam ab16667), E-cadherin (Cell Signaling 3195), BrdU (Abcam ab6326) followed by species specific secondary antibody labeling. HRP was detected using the DAB reaction (DAKO). TUNEL and ISOL staining were performed according to the manufacturer's protocols (MilliporeSigma). Hematoxylin and eosin-stained and immunoperoxidase-stained tissues were imaged using a DMLB microscope (Leica) with 10x HC NA0.25 FL PLAN, 20x NA 0.5 HC PL FLUOTAR, and 40x NA0.65 HC FL PLAN objectives, and MicroPublisher 3.3 or MicroPublisher 5.0 CCD cameras (QImaging) controlled by QCapPro 6. Post-acquisition processing was performed in Adobe Photoshop Lightroom 5.7.

Immunofluorescent staining of paraffin embedded tissue followed deparaffinization and antigen retrieval procedures described above but also included photobleaching (except for TUNEL and ISOL stains).¹⁰ Sections of snap-frozen tissues were fixed with 1% paraformaldehyde in PBS, as described.² Cultured cell monolayers were fixed with 2% paraformaldehyde in PBS before

permeabilization and staining.¹¹ Specimens were stained using the same antibodies as above except that rat monoclonal anti-occludin antibodies (clones 3H5D11, 5E5A6, and 7C2C3) and mouse anti-E-cadherin (clone M168, Abcam ab76055) primary antibodies, Alexafluor-conjugated secondary antibodies (AffiniPure F(ab')₂ fragments, Jackson ImmunoResearch), and fluorogenic TUNEL and ISOL kits were used. Fluorescent-stained specimens were imaged using an Axioplan 2 microscope (Zeiss) with 10x NA0.5 FLUAR, 20x NA0.8 PLAN-APOCHROMAT, 63x NA 1.35 and 100x NA1.30 PLAN-NEOFLUAR objectives and a Coolsnap HQ (Photometrics) camera controlled by Metamorph 7 (Molecular Devices) or a DM4000 microscope (Leica) with 20x NA0.70 HC PLAN APO and 40X NA0.75 HCX PLAN-FLUOTAR objectives and Hamamatsu Flash LT Plus camera controlled by Metamorph 7. Both microscopes were equipped with ET filter cubes (49000, 49002, 49008, and 49009, Chroma Technology). Post-acquisition processing was performed in MetaMorph 7.8.

Intestinal Permeability

Mice were denied access to food but allowed water for 4 h prior to gavage with 0.2 mL saline containing 160 mg fluorescein isothiocyanate-4 kDa dextran (Sigma FD4). Serum was harvested after 4 hr. Recovery of fluorescent probes was measured using 495 nm excitation and 525 nm emission wavelengths using a Synergy H1 multimode plate reader (BioTek).

Epithelial isolation and immunoblots

Small intestinal epithelial cells were isolated using 2 mM EDTA, as described.⁶ The procedure for colonic epithelial cell isolation was similar except that 25 mM EDTA was used. Isolated mouse intestinal epithelial cells or cultured Caco-2_{BBE} monolayers were lysed with non-reducing SDS sample buffer, boiled, separated by SDS-PAGE (Bio-Rad, Hercules, CA, USA), and transferred to nitrocellulose membranes as described.⁸ Membranes were incubated with primary antibodies against occludin (ThermoFisher 33-1500), caspase-3 (Cell Signaling 9662), cleaved caspase-3 (Cell Signaling 9664), GAPDH (ThermoFisher 43-7000), phospho-ERK (p44/42, Cell Signaling 4370), ERK (p44/42, Cell Signaling 4695), phospho-p38 MAP kinase (Cell Signaling 4511), p38 MAP kinase (Cell Signaling 8690), I κ B (Cell Signaling 4814), caspase-8 (Cell Signaling 4790), caspase-9 (Cell Signaling 9508), E-cadherin (Cell Signaling 3195), Apaf-1 (Cell Signaling 8723), cIAP-1 (Cell Signaling 4952), survivin (Cell Signaling 2808), Bax (Cell Signaling 2772), PUMA (Cell Signaling), BID (Cell Signaling 2003), Bcl-xL (Cell Signaling 2764),

Mcl-1 (Cell Signaling 5453), SMAC (Cell Signaling 2954), cytochrome C (Cell Signaling 4280), Bcl-2 (Santa Cruz sc-7382), or XIAP (BD Biosciences 610762) followed by HRP-conjugated secondary antibodies (Cell Signaling). Proteins were detected by chemiluminescence using HYBLOT CL film (Denville) or an Fc gel imaging system (Li-Cor). Densitometry was performed using ImageJ.

RNA isolation and quantitative RT-PCR

RNA was purified from isolated intestinal epithelial cells lysed in Trizol (ThermoFisher) using RNeasy minicolumns (Qiagen). DNA was digested with RNase-free DNase. RNA was then reverse transcribed (New England Biolabs) and analyzed by quantitative real-time PCR using SsoFast Evagreen reagent (Bio-Rad) and a CFX96 thermocycler (Bio-Rad). Primers were: human *CASP3* forward: 5'-TGGACGCAGCCAACCTCAGA-3', reverse: 5'-TCATCACCATGGCTTAGAATCACAC-3'; human *GAPDH*: forward 5'-CTTACCACCATGGAGAAGGC-3', reverse 5'-GGCATGGACTGTGGTCATGAG-3'; mouse *Casp3*: forward: 5'-AAGATACCGGTGGAGGCTGACTTC-3' reverse: 5'-CATGCTGCAAAGGGACTGGATG-3'; mouse *Casp8*: forward: 5'-CTTCGAGCAACAGAACCACA-3' reverse: 5'-TTCTTACCAGTAGCCATTCC-3'; mouse *Gapdh*: forward: 5'-CTTACCACCATGGAGAAGGC-3', reverse: 5'-GGCATGGACTGTGGTCATGAG-3'; mouse *Cdh1*: forward: 5'-TCCTTGTTCCGGCTATGTGTC-3', reverse: 5'-GGCATGCACCTAAGAATCAG-3'; mouse *Krt8*: forward: 5'-CTCCTGCAGCTGTATGGCAG-3', reverse: 5'-AAGGTTGGCCAGAGGATTAGG-3'; mouse *Il6*: forward: 5'-CCGGAGAGGAGACTTCACAG-3', reverse: 5'-TCCACGATTTCCCAGAGAAC-3'; mouse *Tnf*: forward: 5'-AGCCCCAGTCTGTATCCTT-3', reverse: 5'-AGCCCCAGTCTGTATCCTT-3'; mouse *Il1b*: forward: 5'-GAGTGTGGATCCCAAGCAAT-3', reverse: 5'-TACCAGTTGGGGAAGTCTGCTGC-3'; mouse *Il17*: forward: 5'-TTCAGGGTCCGAGAAGATGCT-3', reverse: 5'-AAACGTGGGGTCTTCTTAGG-3'; mouse *Cxcl1*: forward: 5'-TGTTGTGCGAAAAGAAGTGC-3', reverse: 5'-TACAAACACAGCCTCCCACA-3'; mouse *Tjp1*: forward: 5'-TGGAATTGCAATCTCTGGTG-3', reverse: 5'-CTGGCCCTCCTTTAACACA-3'; mouse *Ocln*: forward: 5'-GCTGTGATGTGTGTGAGCTG-3', reverse: 5'-GACGGTCTACCTGGAGGAAC-3'.

Myeloperoxidase activity assay

Myeloperoxidase assay was performed using a previously reported protocol.¹² Briefly, colonic tissues were snap frozen and stored in liquid nitrogen. After homogenization in PBS containing 0.5% hexdecyltrimethylammonium bromide (MilliporeSigma), lysates were clarified by centrifugation and incubated with hydrogen peroxide and O-dianisidine dihydrochloride (1mg/ml) in phosphate buffer. Absorbance was read at 450 nm using a Synergy HT plate reader (BioTek). Purified human myeloperoxidase (MilliporeSigma) was used to construct a standard curve.

Caspase activity

Confluent Caco-2_{BBE} monolayers were isolated in PBS and resuspended in 20 mM HEPES–KOH, pH 7.5, 10 mM KCl, 1.5 mM MgCl₂, 1 mM sodium EDTA, 1 mM sodium EGTA, 1 mM dithiothreitol, with 1 mM α -phenylmethylsulfonyl fluoride, 10 μ g/ml pepstatin A, and 10 μ g/ml leupeptin. Cells were disrupted by using a tight-fitting Dounce homogenizer and debris removed by centrifugation at 800xg. The 100,000xg supernatant was defined as the S100 fraction, of which 50 μ g was incubated at 37°C with or without addition of 1 mM dATP and 50 nM cytochrome C (to activate caspases) before analysis. Fluoregenic caspase substrates, 100 μ M (Ac-IETD-AFC for caspase-8, Ac-LEHD-AFC for caspase-9, Ac-DEVD-AFC for caspase-3, BD Biosciences), were in 20 mM HEPES-KOH, pH 7.5, 0.1% CHAPS were added, and fluorescence was measured using 400 nm excitation and 505 nm emission wavelengths using a Synergy HT plate reader.

Luciferase assay

The 1.8 kb human *CASP3* promoter inserted upstream of firefly luciferase in pGL3¹³ was transiently transfected along with a plasmid encoding *Renilla* luciferase (to normalize for transfection efficiency) into control, occludin KD, or occludin KD with tet-inducible EGFP or EGFP-occludin expression. For mRNA stability assays, the complete human *CASP3* 3'UTR was cloned into the pmirGlo vector (Promega) downstream of firefly luciferase. The plasmid also encodes *Renilla* luciferase to allow normalization for transfection efficiency. Transiently transfected cells were plated onto collagen coated Transwells, cultured for 2-3 weeks, lysed, and analyzed by dual luciferase assay (Promega). Luminescence was determined using a Smart Line TL luminometer (Berthold).

Statistical analysis

All data presented are representative of three or more independent experiments and are shown as mean \pm SD unless otherwise specified. For comparison between two groups with continuous variables, Student's *t*-test was used to compare means. For comparison of multiple groups of samples, one-way ANOVA analysis with Bonferroni post-test was used. To compare discontinuous variables between two groups, Mann-Whitney U test was used. * $P \leq 0.05$, ** $P \leq 0.01$, and n.s., $P > 0.05$. Statistical analyses were performed using Excel (Microsoft) or Prism (GraphPad).

Supplemental References

1. Saitou M, Furuse M, Sasaki H, et al. Complex phenotype of mice lacking occludin, a component of tight junction strands. *Mol Biol Cell* 2000; 11:4131-42.
2. Marchiando AM, Shen L, Graham WV, et al. Caveolin-1-dependent occludin endocytosis is required for TNF-induced tight junction regulation in vivo. *J Cell Biol* 2010; 189:111-26.
3. el Marjou F, Janssen KP, Chang BH, et al. Tissue-specific and inducible Cre-mediated recombination in the gut epithelium. *Genesis* 2004; 39:186-93.
4. Kuida K, Zheng TS, Na S, et al. Decreased apoptosis in the brain and premature lethality in CPP32-deficient mice. *Nature* 1996; 384:368.
5. Odenwald MA, Choi W, Kuo WT, et al. The scaffolding protein ZO-1 coordinates actomyosin and epithelial apical specializations in vitro and in vivo. *J Biol Chem* 2018; 293:17317-17335.
6. Clayburgh DR, Barrett TA, Tang Y, et al. Epithelial myosin light chain kinase-dependent barrier dysfunction mediates T cell activation-induced diarrhea in vivo. *J Clin Invest* 2005; 115:2702-15.
7. Waldner MJ, Neurath MF. Chemically induced mouse models of colitis. *Curr Protoc Pharmacol* 2009; Chapter 5:Unit 5 55.
8. **Buschmann MM, Shen L, Rajapakse H**, et al. Occludin OCEL-domain interactions are required for maintenance and regulation of the tight junction barrier to macromolecular flux. *Mol Biol Cell* 2013; 24:3056-68.
9. Wang F, Graham WV, Wang Y, et al. Interferon-gamma and tumor necrosis factor-alpha synergize to induce intestinal epithelial barrier dysfunction by up-regulating myosin light chain kinase expression. *Am J Pathol* 2005; 166:409-19.
10. Lin JR, Fallahi-Sichani M, Chen JY, et al. Cyclic Immunofluorescence (CyclIF), A Highly Multiplexed Method for Single-cell Imaging. *Curr Protoc Chem Biol* 2016; 8:251-264.
11. Raleigh DR, Boe DM, Yu D, et al. Occludin S408 phosphorylation regulates tight junction protein interactions and barrier function. *J Cell Biol* 2011; 193:565-82.
12. Dalmaso G, Nguyen HT, Ingersoll SA, et al. The PepT1-NOD2 Signaling Pathway Aggravates Induced Colitis in Mice. *Gastroenterology* 2011; 141:1334-45.
13. **Song B, Xie B**, Wang C, et al. Caspase-3 is a target gene of c-Jun:ATF2 heterodimers during apoptosis induced by activity deprivation in cerebellar granule neurons. *Neurosci Lett* 2011; 505:76-81.

Author names in bold designate shared co-first authorship.